Radiotherapy and Oncology 146 (2020) 21–28

Contents lists available at ScienceDirect

Radiotherapy and Oncology

journal homepage: www.thegreenjournal.com

Original Article

# Target motion mitigation promotes high-precision treatment planning and delivery of extreme hypofractionated prostate cancer radiotherapy: Results from a phase II study

Carlo Greco [a,*], Oriol Pares [a], Nuno Pimentel [a], Vasco Louro [a], Javier Morales [a], Beatriz Nunes [a], Ana Luisa Vasconcelos [a], Ines Antunes [a], Justyna Kociolek [a], Joep Stroom [a], Sandra Viera [a], Dalila Mateus [a], Maria Joao Cardoso [a], Ana Soares [a], Joao Marques [a], Elda Freitas [a], Graca Coelho [a], Zvi Fuks [a,b]

[a] The Champalimaud Centre for the Unknown, Lisbon, Portugal; [b] Memorial Sloan Kettering Cancer Center, New York, USA

ARTICLE INFO

*Article history:*
Received 17 November 2019
Received in revised form 26 January 2020
Accepted 30 January 2020
Available online 19 February 2020

*Keywords:*
SBRT
Extreme hypofractionation
Prostate cancer
Motion mitigation
Urethral sparing
Quality of life

ABSTRACT

*Background and purpose:* While favourable long-term outcomes have been reported in organ-confined prostate cancer treated with 5 × 7–8 Gy extreme hypofractionation, dose escalation to 5 × 9–10 Gy improved local control but was associated with unacceptable rates of late rectal and urinary toxicities. The purpose of this study was to explore the feasibility of intra-fractional prostate immobilization in reducing toxicity, to promote dose escalation with extreme hypofractionated radiotherapy in prostate cancer.

*Material and methods:* 207 patients received 5 consecutive fractions of 9 Gy. An air-inflated (150 $cm^3$) endorectal balloon and an intraurethral Foley catheter with 3 beacon transponders were used to immobilize the prostate and monitor intra-fractional target motion. VMAT-IGRT with inverse dose-painting was employed in delivering the PTV dose and in sculpting exposure of normal organs at risk to fulfil dose-volume constraints.

*Results:* Introduction of air-filled balloon induced repeatable rectum/prostate complex migration from its resting position to a specific retropubic niche, affording the same 3D anatomical configuration daily. Intra-fractional target deviations ≤1 mm occurred in 95% of sessions, while target realignment in ≥2 mm deviations enabled treatment completion as scheduled. Nadir PSA at median 54 months follow-up was 0.19 ng/mL, and bRFS was 100%, 92.4% and 71.4% in low-, intermediate- and high-risk categories, respectively. Late Grade 2 GU and GI toxicities were 2.9% and 2.4%, respectively. No adverse changes in patient-reported quality of life scores were observed.

*Conclusion:* The unique spatial configuration of this prostate motion mitigation protocol enabled precise treatment planning and delivery that optimized outcomes of ultra-high 5 × 9 Gy hypofractionated radiotherapy of organ-confined prostate cancer.



The general aim of extreme hypofractionated Stereotactic Body Radiotherapy (SBRT) of prostate cancer (PCa) is to leverage the unique radiobiological attributes of PCa to improve treatment efficacy, cost effectiveness and patient satisfaction [1]. Evidence indicates that the linear quadratic α/β ratio of PCa is generally lower than in the majority of other human tumors, even lower than the α/β ratio of late-responding normal tissues [2,3]. These observations imply that extreme hypofractionation with a small number of large fractions may have a radiobiological advantage in rendering PCa tumor cure with limited toxicity [2]. There is a large body of literature confirming this model in all PCa risk categories, mostly engaging SBRT schedules of 5 × 7–8 Gy/fraction [1]. The Scandinavian HYPO-RT-PC phase 3 randomized study provided proof-in-principle of non-inferiority in the therapeutic outcomes of extreme hypofractionation (7 × 6.1 Gy) when compared with conventional fractionated 78 Gy in 39 fractions [4]. An extreme hypofractionated phase II study reported 515 patients treated with 5 × 7–7.25 Gy/fraction yielding 8-year disease-free survival rates of 93.6%, 84.3%, and 65.0% in low- intermediate-, and high-risk patients, respectively. Late Grade 2–3 GU toxicities were 9.1% and 1.7%, respectively, while Grade 2 GI toxicity was 4% [5,6]. Another recent study in 551 low- and intermediate-risk PCa patients employing 5 fractions of 7.5 Gy or 8 Gy yielded an overall 5-year cumulative incidence of PSA failure of only 2.1% and low rates of Grade 2 GU

* Corresponding author at: Department of Radiation Oncology, Champalimaud Centre for the Unknown, Avenida Brasilia s/n, 1400-038 Lisbon, Portugal.
*E-mail address:* carlo.greco@fundacaochampalimaud.pt (C. Greco).

https://doi.org/10.1016/j.radonc.2020.01.029
0167-8140/

and GI toxicities [7]. However, 119 patients received a post treatment biopsy revealing a positive biopsy incidence of 17.9% and 9.9% after 37.5 Gy and 40 Gy respectively [7], suggesting an indication for dose escalation to maximize the likelihood of local tumor control. However, while a previous phase I/II trial reported high rates of 98.6% 5-year bRFS in 91 patients treated with local tumor control 5 fractions of 9–10 Gy, it was associated with unacceptable late Grade 3–4 rectal and urinary toxicities [8].

The latter observations indicate that at the high end of hypofractionated biological equivalent dose (BED) levels, the low $\alpha/\beta$ ratio advantage in normal tissue sparing is exceeded. While enhanced accuracy in target dose deposition, implementation of sharp penumbra dose gradients, and use of hydrogel rectal spacers have reduced rectal toxicity [9], these maneuvers only partially resolve the baseline toxicity issues associated with high-end BED levels of PCa SBRT. The prostate is a highly mobile organ due to its location in the spatially tight pelvic outlet, affected by rectal or urinary bladder fillings, deforming and displacing the prostate [10]. Prostate mobility studies using beacon transponder technology showed that approximately 20% of PCa patients exhibit major 3–10 mm intra-fractional prostate displacements during treatment delivery [11–13], associated with OAR over-exposure and/or under-exposure of the target. Hence, target motion mitigation has become a focus of clinical research in prostate cancer radiotherapy with extreme hypofractionation [13].

Here we report an experimental approach to immobilize the prostate during treatment with extreme 5 × 9 Gy hypofractionation (mean PTV dose 45.8 Gy) delivered in 5 consecutive days. The study was based on a working hypothesis that intra-fractional target immobilization is a conditional prerequisite for high precision delivery of a curative target dose with concomitant dose-sculpted exposures of the relevant OARs (i.e. bladder neck, urethra, rectal wall and the neurovascular bundles). Techniques for reproducible prostate and OARs motion mitigation have not been reported thus far, although a large body of literature indicates that inflated endorectal balloons reduce intrafraction prostate motion [14–16]. Balloon air filling has generally been restricted to 40–100 $cm^3$ to avoid patients' discomfort [16–18]. However, Wang et al. [19] demonstrated that a 100 $cm^3$ still permits bypass of gas and stool around the balloon, allowing limited, albeit measurable, prostate mobility. The present study explored the feasibility of increasing the air-volume of the endorectal balloon to 150 $cm^3$, the threshold of tolerable rectal filling [20]. Patients were also asked to void immediately prior to simulation and each treatment session. A Foley catheter containing beacon transponders was introduced at every session to provide non-invasive on-line organ motion tracking, also aiding in segmentation and targeting the whole length of the prostatic urethra for dose reduction. A primary endpoint of this study was to test whether this immobilization protocol provides a potential for improved precision in treatment planning and delivery. The early-phase actuarial biochemical relapse-free survival, acute and late toxicity profiles and the patient-reported quality of life (QoL) post-therapy, underscore the highly favourable outcomes of this therapeutic approach.

## Materials and methods

### Patients

A total of 207 patients with organ-confined prostate adenocarcinoma, an IPSS score ≤15 and an estimated gland volume of ≤100 grams were included in this IRB approved phase 2 study (clinicaltrials.gov NCT02761889) between June 2013 and May 2017. Patients characteristics are shown in Table 1. Median follow-up time was 54 months (range 30–78 months; Interquartile range [IQR] 41.6–64.6). Two patients died of comorbidities without evidence of disease, and 15 were lost to follow-up at a median time of 22 months.

**Table 1**
Patients and tumor characteristics.

| Patient and tumor characteristics | ($n$ = 207) | |
|---|---|---|
| *Age (years)* | | |
| median | 70.1 | |
| mean | 68.9 | |
| range | 44.5–89.8 | |
| *Gland size ($cm^3$)* | | |
| median | 44.1 | |
| Mean | 49.4 | |
| range | 11.1–118.9 | |
| *Pretreatment PSA (ng/mL)* | | |
| median | 7.1 | |
| mean | 8.3 | |
| range | 1.9–19.3 | |
| *Pretreatment PSA* | | |
| <10 ng/mL | 150 | 72% |
| ≥10 ng/mL | 57 | 28% |
| *IUSP Grade* | | |
| Group 1 | 37 | 18% |
| Group 2 | 111 | 54% |
| Group 3 | 51 | 24% |
| Group 4 | 8 | 4% |
| *T-stage* | | |
| T1c | 28 | 13% |
| T2a | 78 | 39% |
| T2b | 46 | 22% |
| T2c | 55 | 26% |
| *Risk group* | | |
| Low | 18 | 9% |
| Intermediate | 176 | 85% |
| High | 13 | 6% |
| *Intermediate risk* | | |
| Favorable | 117 | 56% |
| Unfavorable | 59 | 29% |
| No ADT | 151 | 73% |
| ADT | 56 | 26% |

Patients were stratified according to NCCN criteria. At the discretion of the referring physician, 56 of the intermediate-risk patients with ISUP Grade Group 3 or patients in the high-risk category received androgen deprivation therapy (ADT) for a maximum of 6 months, but ADT was discontinued upon acceptance to the study. All participants signed an informed consent prior to study participation.

### Treatment planning and radiation delivery

Following a rectal enema and bladder voiding, patients were simulated in a supine position with a leg fixation device. A set of 3 beacon transponders embedded in a 12 French gauge Foley catheter (4 mm diameter) was used for intra-fractional tracking (Calypso®, Varian Medical Systems, Palo Alto, CA). The Foley catheter also guided the segmentation of the whole length of the prostatic urethra for dose reduction and for treatment and was present at every session, be it simulation, planning or actual treatment delivery. An endo-rectal balloon (Rectal Pro, QLRAD Inc., FL) was inflated with 150 $cm^3$ of air while inside the rectal ampulla. A CT and a T2W 3D MR scans were acquired and fused to delineate the target volume and OARs. The PTV consisted of the CTV (the prostate and the proximal two-thirds of the seminal vesicles) with a 2 mm isotropic 3D margin. The margin was reduced to 0 mm at the rectal wall, the bladder, UGD and urethra wall (defined as a 2 mm expansion around the catheter). Plan objectives are summarized in Table 2. The study employed an experimental approach to

**Table 2**
Plan dosimetric results.

| Plan dosimetric results | median | mean | range | plan objective |
|---|---|---|---|---|
| *PTV* | | | | |
| $D_{50\%}$ (Gy) | 46.6 | 46.6 | 46.0–47.9 | ≥45.0 |
| $D_{mean}$ (Gy) | 45.9 | 45.8 | 42.9–46.9 | ≥45.0 |
| $D_{95\%}$ (Gy) | 40.7 | 40.4 | 35.8–43.6 | ≥40.5 |
| $D_{2\%}$ (Gy) | 47.9 | 47.4 | 47.3–49.0 | ≤48.2 |
| $D_{98\%}$ (Gy) | 38.7 | 38.2 | 34.8–41.4 | ≥38.2 |
| $V_{45Gy}$ (%) | 81.4 | 81.1 | 72.6–91.5 | ≥80 |
| $V_{40.5Gy}$ (%) | 95.3 | 94.7 | 86.3–98.6 | ≥95 |
| *Urethral wall* | | | | |
| $D_{2\%}$ (Gy) | 38.8 | 38.7 | 36.7–41.9 | |
| $D_{1cm^3}$ (Gy) | 34.6 | 33.9 | 9.8–35.9 | ≤36.0 |
| *Bladder* | | | | |
| $D_{2\%}$ (Gy) | 37.5 | 37 | 28.2–40.6 | |
| $D_{50\%}$ (Gy) | 14.5 | 12.6 | 0.8–22.3 | ≤22.5 |
| $D_{1cm^3}$ (Gy) | 39.1 | 38.7 | 30.6–40.4 | ≤40.5 |
| *Rectal wall* | | | | |
| $D_{2\%}$ (Gy) | 36.4 | 36.3 | 31.9–38.3 | |
| $D_{5\%}$ (Gy) | 33.3 | 32.7 | 23.5–35.2 | ≤40.5 |
| $D_{50\%}$ (Gy) | 10.9 | 10.3 | 1.2–21.2 | ≤22.5 |
| $D_{1cm^3}$ (Gy) | 35.3 | 35.2 | 31.1–35.9 | ≤36.0 |
| *UGD* | | | | |
| $D_{2\%}$ (Gy) | 37.9 | 35.7 | 9.5–42.9 | ≤42.8 |
| *Penile bulb* | | | | |
| $D_{2\%}$ (Gy) | 2.5 | 3.7 | 0.9–33.6 | <36.0 |
| $D_{1cm^3}$ (Gy) | 1.6 | 2.2 | 0.8–22.4 | ≤22.5 |
| *NVBs* | | | | |
| $D_{2\%}$ (Gy) | 39.8 | 41.3 | 38.2–47.8 | <45.0 |
| *Femoral heads* | | | | |
| $D_{2\%}$ (Gy) | 12.9 | 12.8 | 5.5–20.9 | ≤22.5 |

*Abbreviations:* PTV, Planning Target Volume; $D_{mean}$, mean dose; $D_{2\%}$, $D_{5\%}$, $D_{50\%}$, $D_{95\%}$, $D_{98\%}$, minimum dose to n% of the structure; $V_{45Gy}$, $V_{40.5Gy}$, percentage of structure receiving 45 Gy or 40.5 Gy (100% and 90% of the prescription dose); $D_{1cm3}$, dose to 1 $cm^3$ of the structure; UGD, urogenital diaphragm; NVB, neurovascular bundles.

render urethral sparing, using a rigidly fixed urethra by the Foley catheter at every treatment session and by inverse dose-painting over a 2 mm expansion around the urethral mucosa visualized by the catheter, with the aim of reducing the dose to the urethral wall by 20%.

Plans were optimized using penalties to control PTV dose coverage and dose constraints to OARs with the progressive resolution optimizer (PRO v10.0.28–v13.7.14 in Eclipse, Varian Medical Systems, Palo Alto, CA) and calculated with the analytical anisotropic algorithm (AAA v10.0.28–v13.7.14). A 10 MV FFF beam energy and 4 VMAT arcs were used in all cases. Treatment was delivered on a linear accelerator with a 2.5 mm leaf width HDMLC (TrueBeam STx or EDGE, Varian Medical Systems, Palo Alto, CA). Treatment plans were quality assured before the first treatment session using an ArcCHECK phantom (Sun Nuclear Corp. FL) to confirm they fulfilled the gamma (3%/3mm) passing rate >90% objective according to AAPM guidelines.

Patient set-up and target localization were achieved by CBCT matching. If discrepancies of ≥1 mm in translation or ≥1 degree in rotation were detected, corrections were applied via a 6-degrees of freedom couch (PerfectPitch 6-DoF Couch, Varian Medical Systems, Palo Alto, CA). Treatment was interrupted when beacon-transponder signals threshold exceeded a 2 mm deviation and treatment target position was re-defined by repeat CBCT. Dose distributions at mid-prostate representative of the typical plan with the urethral inverse dose painting are shown in Fig. 1.

### *Toxicity and quality of life assessment*

Toxicity (NCI CTCAE v.4.0) was assessed post-treatment at one month and every 3–12 months (±4 weeks), and at every 6 months thereafter. IPSS and EPIC-26 forms were collected at baseline and at the same time points post-treatment as above.

### *Statistical methods*

Actuarial biochemical-free PSA survival (bRFS), GU and GI toxicities, and QoL scores were computed from the end of treatment using the Kaplan-Meier method. Student's *t*-test and chi-square analysis were used to assess differences in PSA, and QOL scores. For each EPIC domain, the levels of responses were assigned a score and the significance of the mean changes was assessed by paired *t*-test and analysis of variance (ANOVA). Univariate analysis of relevant variables was performed using the Cox proportional hazards regression method. Hazard ratio (HR), 95% confidence intervals (CI) were obtained and the level of statistical significance was set at 0.05. Statistical computations were performed using the GraphPad *Prism 7.0* software (Prism Inc, Reston, VA).

## Results

A total 207 patients were accrued to the study (Table 1). While a 150 $cm^3$ endorectal air-inflated balloon volume was chosen to immobilize the prostate based on published tolerance data [20] we, nonetheless, quality assured the tolerance of the balloon volume. In the first 15 patients at the time of simulation the balloon was filled with increasing volumes of air (0, 50, 100, 150, 200 and 250 $cm^3$) (Fig. 1A, B), confirming that 150 $cm^3$ was the maximally tolerated volume, as two patients reported major discomfort at 200 $cm^3$. All of the 207 patients were treated with the chosen 150 $cm^3$ volume.

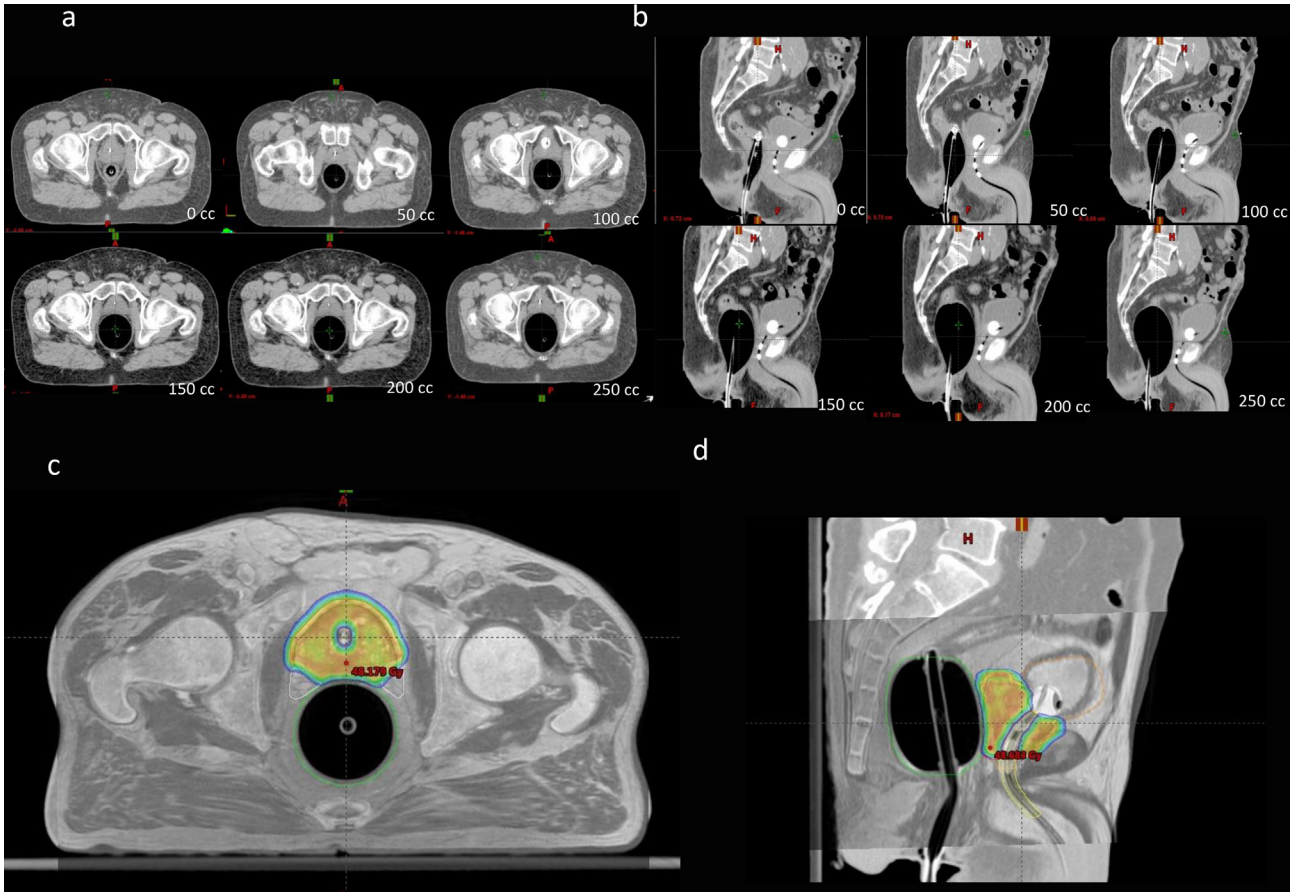


**Fig. 1.** Target immobilization in prostate cancer. (A-B) show a balloon inflation volume escalation study (0 to 250 $cm^3$) on the axial (A) and sagittal (B) planning CT planes. The An intraurethral Foley catheter loaded with 3 beacon transponders is visible on the longitudinal planes. (C-D) show fused CT-MR image sets with dose-sculpted distributions along the urethra, rectal wall, urogenital diaphragm and neurovascular bundles.

The intra-fractional treatment accuracy in the interval between reference CBCT acquisition to treatment end was systematically analysed. A mean of 2.5 CBCT/planning CT matchings (median 2; IQR 2–3) were employed. Mean total dose delivery time was 5 min. Target geometrical variations during treatment delivery were limited to $\leq$1 mm in 95% of treatment sessions. Treatment interruptions were required in 5% due to beacon-transponder-identified drifts of >2 mm for $\geq$5 s, enabling treatment completion as planned in all instances. Analysis of beacon motion during treatment delivery in 63 consecutive patients yielded position uncertainties of 0.4 mm to 0.6 mm (1SD) in all directions.

Furthermore, evaluations of inter-fractional variations in prostate localization and anatomical prostate deformation assessed in 38 patients showed that the average standard deviation for distances between Foley entrance or beacons and the rectal balloon was 1.0 mm, and to the pubic bone 0.8 mm. Laterally, values were similar with SDs and ranges for left and right 0.8 mm and 0.9 mm, respectively. SDs were calculated from an average 10 CBCTs per patient. These data constituted a basis for the study-specific isotropic 2 mm CTV to PTV margin expansion and confirmed that the prostate reproducibly occupies the same anatomical niche at each fraction.

Following treatment, PSA gradually decreased to a median of 0.19 ng/mL at 48 months (Fig. 2a). Median nadir PSA (nPSA) was 0.19 ng/mL (mean 0.56; range 0.04–3.8; IQR 0.07–0.4). Patients who experienced a biochemical relapse had a higher median nPSA (0.9 ng/mL; IQR 0.8–1.2) compared to that of those who did not (median 0.2 ng/mL; IQR 0.1–0.38) ($p < 0.001$). Using the nadir + 2 (Phoenix definition) the actuarial bRFS at the median 54 months follow-up was 91.8% for the entire cohort (Fig. 2b), and 100%, 92.4% and 71.4% for the NCCN low-, intermediate- and high-risk groups, respectively (Fig. 2c).

Analysis of favourable and unfavourable intermediate-risk categories revealed significantly different actuarial bRFS (100% vs 88.9% respectively; $p = 0.028$) (Fig. 2d). Initial biopsy Grade Group was associated with bRFS outcome with Grade Groups 1, 2, and 3 having 100%, 94.6%, 81.9% bRFS, respectively ($p = 0.002$) (Fig. 3a), as was baseline PSA $\geq$10 vs <10 ng/mL (91.3% vs 84.8%: $p = 0.022$) (Fig. 3b). The use of a maximum of 6 months ADT was not associated with bRFS probability ($p = 0.8$) (Fig. 3D), or MR-based clinical T stage (T1c-T2a vs T2b-T2c; 93.6% vs 90.4%; $p = 0.6$) (Fig. 3C).

Median time to nPSA was 36 months (IQR 30–48). The majority of patients in this cohort (195/207; 94%) reached a nPSA <1 ng/mL, while 80% (166/207) and 50% (103/207) reached an nPSA of <0.5 ng/mL and <0.2 ng/mL, respectively. A nPSA of <0.2 ng/mL was strongly associated with improved bRFS (100% vs 85.4%; $p = 0.005$). Benign PSA bounces were observed in 36% (75/207) of patients with a median magnitude of 0.50 ng/mL (IQR 0.3–1.2) and a median time to bounce of 12 months (IQR 9.18). Actuarial bRFS at 54 months was 97.8% vs 88.8%, respectively, for patients who experienced a bounce vs those who did not ($p = 0.05$).

No Grade 3 or greater acute or late toxicity was recorded. Twenty-one patients (10.1%) experienced at least one Grade 2 GU toxicity event, mainly consisting of increased urgency and frequency. Six patients (2.9%) developed Grade 2 late GU toxicity.

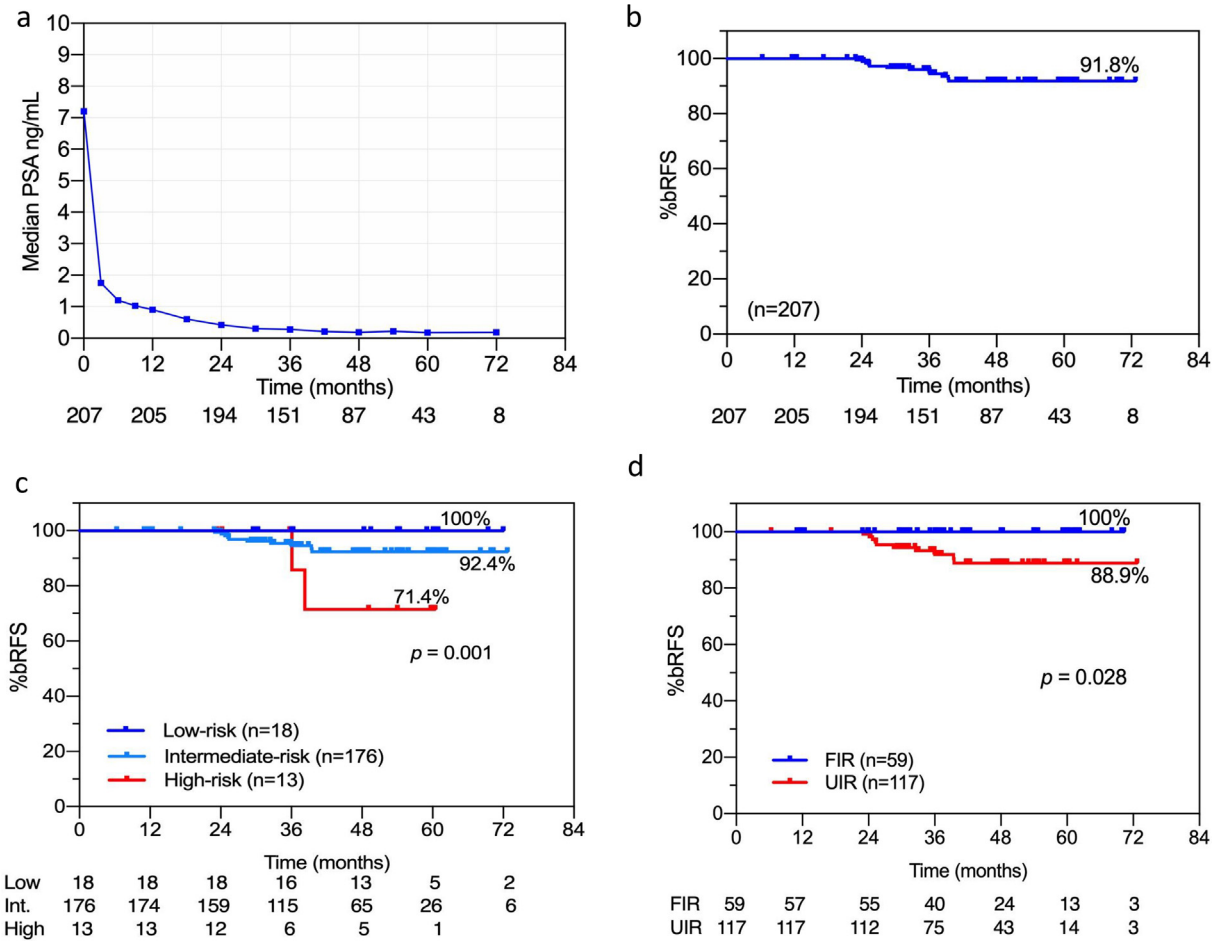


**Fig. 2.** Prostate-specific antigen (PSA) response. (A) Shows median PSA as function of time after treatment and (B-D) PSA relapse-free survival (bRFS) at 5-years. Actuarial bRFS for the entire population (B), for NCCN low-, intermediate- and high-risk groups (C) and NCCN favorable vs. unfavorable intermediate-risk groups (D).

No patients required catheterization for late urinary obstructive symptoms. Thirteen (6.2%) patients developed acute Grade 2 GI toxicity and five (2.4%) patients experienced late Grade 2 rectal toxicity.

The median IPSS increased from 7 at baseline to 11 ($p < 0.001$) 1 month after treatment (Fig. 4a), indicating worsening of obstructive symptoms, but returned to 6 at 3 months post-treatment ($p = 0.89$), approximating the pre-treatment baseline up to 60 months on ANOVA ($p = 0.22$). Patients with larger glands (>50 $cm^3$) had the highest pre-treatment IPSS but showed a better urinary symptom trend than those with smaller volumes, with improved post-treatment IPSS from baseline at one year ($p = 0.001$), confirmed on ANOVA at 48 months ($p = 0.02$).

Similarly, urinary EPIC-26 scores significantly decreased from a median baseline of 89 pre-treatment to 77 at 1 month ($p < 0.0001$) returning to 90 at 3 months post-treatment ($p = 0.57$) (Fig. 4b). Of note, there was a statistically significant drop in the EPIC GU score at 12 months (paired *t* test baseline *vs* 12 months $p = 0.0003$) indicating a pelvic floor flare-up, but scores returned to baseline at later time-points (median score of 89 at 48 months; paired *t* test $p = 0.11$). There was a significant decrease at 1 month in median EPIC-26 GI scores ($p < 0.0001$) resuming to baseline values by 3 months ($p = 0.16$) (Fig. 4C). Median EPIC-26 scores in the sexual domain showed a non-significant drop at 24 months ($p = 0.09$) and statistically significant decreased scores at 36 ($p = 0.01$) and 48 ($p = 0.02$) months (Fig. 4d). These encouraging results are likely due to the attempt to spare the NVB and all other periprostatic vascular structures involved in the erectile function.

## Discussion

The present study defines an approach to induce translocation of the prostate/rectum complex from its natural resting state at the inferior-posterior section of the pelvic diaphragm to a patient-specific anterior retropubic niche, immobilizing the prostate with millimetric precision. The daily relocation of the prostate at the same anatomical configuration was proven by direct measurements of the distances between Foley entrance and/or beacons to the rectal balloon and the pubic bone. Hence, the prostate immobilization protocol converted extreme hypofractionated PCa SBRT into a high-precision plan-and-treat operation.

The preliminary outcomes at a median follow-up of 54 months are encouraging. The median nPSA of 0.19 ng/mL and other PSA kinetics parameters are comparable with published results of extreme hypofractionation in PCa [21–23]. Our PSA kinetic data are in line with the study of Jiang et al. [24], reporting 1062 PCa patients treated with 5 × 7–8 Gy SBRT at median of 66 months, a median follow-up 12 months longer than the present patient cohort. Of note, at the time of last follow-up no biochemical failures were observed in our low-risk and favourable intermediate-risk (FIR) patients (Fig. 2c, d), compared to 1.4% and 6.3%, respectively, reported by Jiang [24], consistent with the higher BED employed in our study. Also, the low GU and GI toxicity profiles in the present study, with no Grade ≥3 toxicities, is are encouraging relative to reported outcomes of 5 × 9–10 Gy schedules [8]. Of special note are our patient-reported QoL outcomes of no adverse changes of IPSS, or EPIC-26 scores in the urinary and bowel

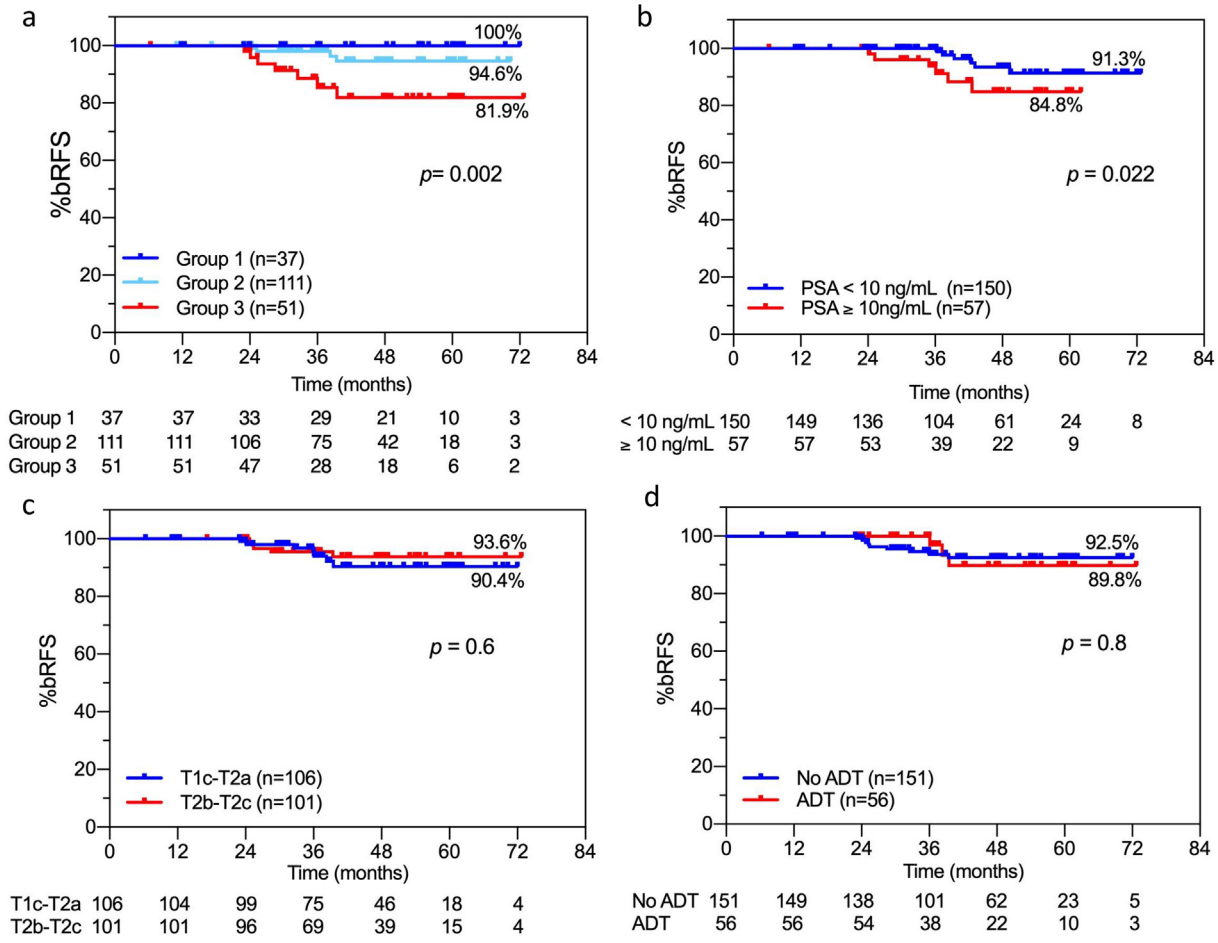


**Fig. 3.** Actuarial bRFS. Analysis is shown as a function of ISUP Grade Group (A), pretreatment PSA (B), clinical disease stage (C) and use of pretreatment androgen deprivation therapy (ADT) (D).

domains, although there are transient declines in EPIC GU and GI QoL at one-month post-treatment, returning to normal baseline values by 3 months. The encouraging sexual QoL outcomes are likely due to the planning efforts to spare the NVB periprostatic vascular structures.

Target relocation at the exact same anatomical niche daily indicates that prostate motion is not stochastic and is likely elicited by a specific physiological mechanism. Consistent with this notion, Lin et al. reported that intra-fractional prostate motion exhibited a non-Gaussian pattern [25], resulting in a phenotypic oblique superior-anterior (SA) axis of motion. A large body of literature supports this model, demonstrating that SA motion dominates the pattern of intrafraction prostate mobility [26–29], and prolonged cine-MRI studies provided evidence for a correlation between rectal filling and coordinated SA prostate motion [30–32]. Mah et al. reported that high-volume gas passing through the rectum induces a rectal peristalsis associated with a SA translocation of the prostate [12], subsequently returning to its steady state localization at the inferior-posterior section of the pelvic diaphragm [12]. Taken together, these observations suggest that rectal wall distension may activate neuronal efferent signals that couple rectal function with prostate motion. Broens et al. [20], while exploring the physiology of defecation, reported that patient sensations of rectal distention differ by the volume of an air-inflated balloon. A distinct, albeit tolerable, sensation of rectal fullness was reported at 150 $cm^3$, and conversion into an intolerable urge begins as of ~200 $cm^3$ [20,33]. While little is known on the efferent neural loops of ano-rectal physiology, cerebral MRI functional studies demonstrated that distinct cortical areas process rectal versus anal stretch stimuli [34], supporting the notion that mechanoreceptor neuronal pathways are associated with rectal stretch sensation.

We posit here that the prostate migration may mimic specific segments of the physiological mechanism of gas movement through the rectum [12]. Whereas the rectum and prostate represent a unique anatomical complex via adhering to the Denonvilliers' fascia [35], it is reasonable to assume that the prostate would be a bystander to rectal mobility induced by peristalsis-mediated progression of intrarectal gas. Rectal shifts are known to occur as part of normal rectal function, coordinated by somatic innervation loops of the *levator ani* muscle system [33]. The *levator ani puborectalis* creates a sling behind the anorectal junction [25,36]. Under baseline conditions the *puborectalis* is permanently contracted blocking the anorectal junction [36,37]. When rectal wall stretch signals are induced by migrating intestinal contents, the *puborectalis* relaxes [33,36], launching a rectal/prostate migration in a SA trajectory [33,36]. Future research is required to address this testable hypothesis using human pelvic imaging to register the sequence of events, as described [37].

In conclusion, the prostate immobilization technique is designed to overcome targeting uncertainties in PCa SBRT. The present studies provide compelling evidence that immobilization enables application of state-of-the-art high precision, image-guided intensity modulated PCa radiotherapy. We suggest that appropriate implementation of the prostate immobilization protocol is a prerequisite to deployment of advanced PCa radiation cura-

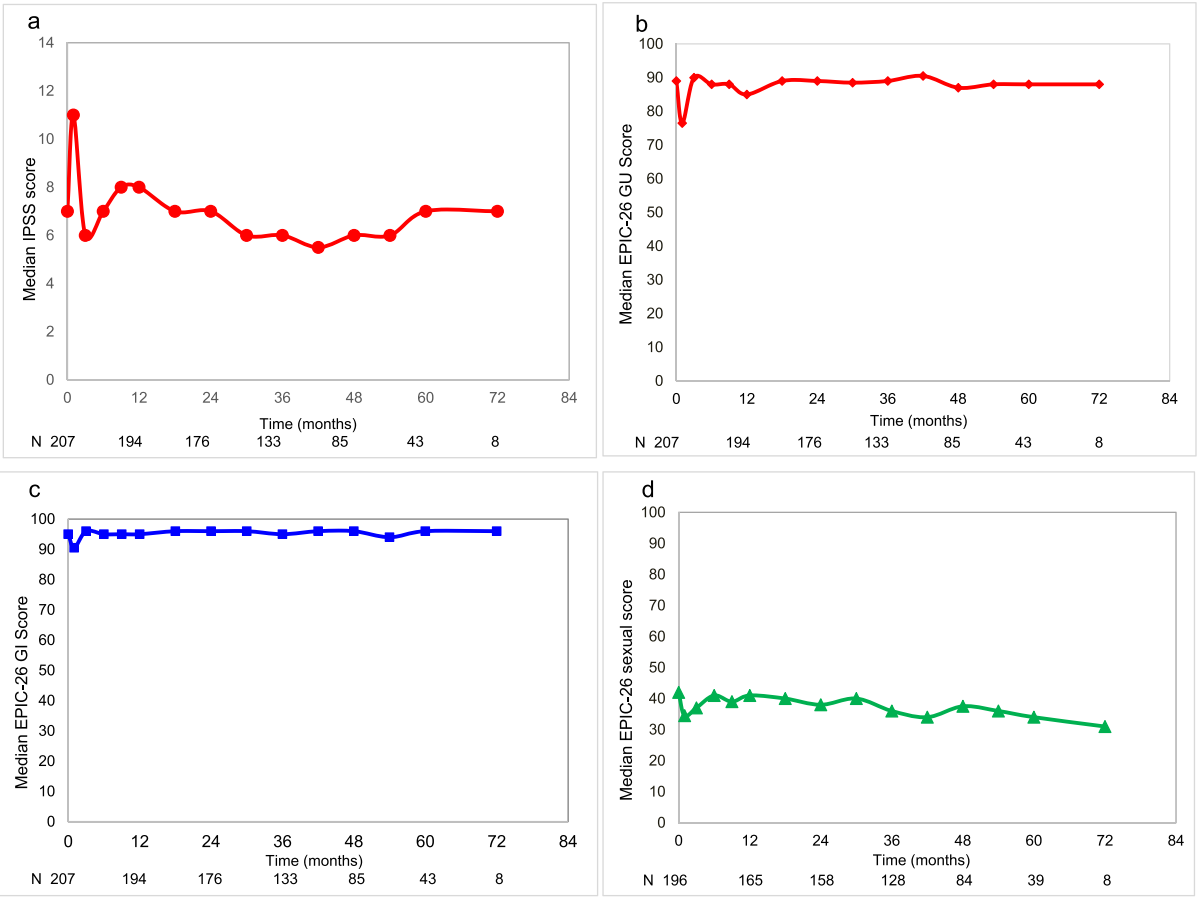


**Fig. 4.** Patient reported outcomes using validated questionnaires (IPSS and EPIC-26) as a function of time post radiotherapy. (A) Median IPSS, (B) EPIC scores of the urinary (B) bowel (C) and sexual (D) domains. EPIC scores range from 0–100 with higher values representing a more favorable health-related QoL.

tive regimens, such as single dose radiotherapy (SDRT), currently underway (PROSINT II, clinicaltrials.gov NCT04035642) leveraging the unique SDRT radiobiology [38].

## Conflict of interest

Patents unrelated to this work for Zvi Fuks (US7195775B1, US7850984B2, US10052387B2, US8562993B2, US95 92238B2, US20150216971A1, US20170335014A1, US20170333413A1, and US20180015183A1) and Carlo Greco (US2018/014639).

The remaining authors have declared no conflicts of interest.

## Funding source

No external funding.

## References

[1] Greco C, Vazirani AA, Pares O, Pimentel N, Louro V, Morales J, et al. The evolving role of external beam radiotherapy in localized prostate cancer. Semin Oncol 2019:1–8. https://doi.org/10.1053/j.seminoncol.2019.08.001.

[2] Proust-Lima C, Taylor JMG, Sécher S, Sandler H, Kestin L, Pickles T, et al. Confirmation of a low α/β ratio for prostate cancer treated by external beam radiation therapy alone using a post-treatment repeated-measures model for PSA dynamics. Int J Radiat Oncol Biol Phys 2011;79:195–201. https://doi.org/10.1016/j.ijrobp.2009.10.008.

[3] Fowler JF, Toma-Dasu I, Dasu A. Is the α/β ratio for prostate tumours really low and does it vary with the level of risk at diagnosis?. Anticancer Res 2013;33:1009–12.

[4] Widmark A, Gunnlaugsson A, Beckman L, Thellenberg-Karlsson C, Hoyer M, Lagerlund M, et al. Ultra-hypofractionated versus conventionally fractionated radiotherapy for prostate cancer: 5-year outcomes of the HYPO-RT-PC randomised, non-inferiority, phase 3 trial. Lancet 2019;394:385–95. https://doi.org/10.1016/S0140-6736(19)31131-6.

[5] Katz AJ, Santoro M, Diblasio F, Ashley R. Stereotactic body radiotherapy for localized prostate cancer: disease control and quality of life at 6 years. Radiat Oncol 2013;8:1. https://doi.org/10.1186/1748-717X-8-118.

[6] Katz A, Formenti SC, Kang J. Predicting biochemical disease-free survival after prostate stereotactic body radiotherapy: risk-stratification and patterns of failure. Front Oncol 2016;6:1–7. https://doi.org/10.3389/fonc.2016.00168.

[7] Zelefsky MJ, Pinitpatcharalert A, Kollmeier M, Goldman DA, McBride S, Gorovets D, et al. Early tolerance and tumor control outcomes with high-dose ultrahypofractionated radiation therapy for prostate cancer. Eur Urol Oncol 2019:1–8. https://doi.org/10.1016/j.euo.2019.09.006.

[8] Hannan R, Tumati V, Xie XJ, Cho LC, Kavanagh BD, Brindle J, et al. Stereotactic body radiation therapy for low and intermediate risk prostate cancer – Results from a multi-institutional clinical trial. Eur J Cancer 2016;59:142–51. https://doi.org/10.1016/j.ejca.2016.02.014.

[9] Jones A, Lyons N, Salter E, Thompson P, Tidball S, Blaikie J, et al. Europe PMC funders group patient-reported outcomes after monitoring surgery, or radiotherapy for prostate cancer. N Engl J Med 2017;375:1425–37. https://doi.org/10.1056/NEJMoa1606221.Patient-Reported.

[10] Langen KM, Jones DTL. Organ motion and its management. Int J Radiat Oncol Biol Phys 2001;50:265–78. https://doi.org/10.1016/S0360-3016(01)01453-5.

[11] Sihono DSK, Ehmann M, Heitmann S, von Swietochowski S, Grimm M, Boda-Heggemann J, et al. Determination of intrafraction prostate motion during external beam radiation therapy with a transperineal 4-dimensional ultrasound real-time tracking system. Int J Radiat Oncol Biol Phys 2018;101:136–43. https://doi.org/10.1016/j.ijrobp.2018.01.040.

[12] Mah D, Freedman G, Milestone B, Hanlon A, Palacio E, Richardson T, et al. Measurement of intrafractional prostate motion using magnetic resonance imaging. Int J Radiat Oncol Biol Phys 2002;54:568–75. https://doi.org/10.1016/S0360-3016(02)03008-0.

[13] Ballhausen H, Li M, Hegemann NS, Ganswindt U, Belka C. Intra-fraction motion of the prostate is a random walk. Phys Med Biol 2015;60:549–63. https://doi.org/10.1088/0031-9155/60/2/549.

[14] McGary JE, Teh BS, Butler EB, Grant W. Prostate immobilization using a rectal balloon. J Appl Clin Med Phys 2002;3:6–11. https://doi.org/10.1120/jacmp.v3i1.2590.

[15] D'Amico AV, Manola J, Loffredo M, Lopes L, Nissen K, O'Farrell DA, et al. A practical method to achieve prostate gland immobilization and target verification for daily treatment. Int J Radiat Oncol Biol Phys 2001;51:1431–6. https://doi.org/10.1016/S0360-3016(01)02663-3.
[16] Wang KKH, Vapiwala N, Deville C, Plastaras JP, Scheuermann R, Lin H, et al. A study to quantify the effectiveness of daily endorectal balloon for prostate intrafraction motion management. Int J Radiat Oncol Biol Phys 2012;83:1055–63. https://doi.org/10.1016/j.ijrobp.2011.07.038.
[17] Van Lin ENJT, Hoffmann AL, Van Kollenburg P, Leer JW, Visser AG. Rectal wall sparing effect of three different endorectal balloons in 3D conformal and IMRT prostate radiotherapy. Int J Radiat Oncol Biol Phys 2005;63:565–76. https://doi.org/10.1016/j.ijrobp.2005.05.010.
[18] Smeenk RJ, Teh BS, Butler EB, van Lin ENJT, Kaanders JHAM. Is there a role for endorectal balloons in prostate radiotherapy? A systematic review. Radiother Oncol 2010;95:277–82. https://doi.org/10.1016/j.radonc.2010.04.016.
[19] Wang KKH, Vapiwala N, Bui V, Deville C, Plastaras JP, Bar-Ad V, et al. The impact of stool and gas volume on intrafraction prostate motion in patients undergoing radiotherapy with daily endorectal balloon. Radiother Oncol 2014;112:89–94. https://doi.org/10.1016/j.radonc.2014.05.008.
[20] Broens PMA, Penninckx FM, Lestár B, Kerremans RP. The trigger for rectal filling sensation. Int J Colorectal Dis 1994;9:1–4. https://doi.org/10.1007/BF00304291.
[21] Kothari G, Loblaw A, Tree AC, van As NJ, Moghanaki D, Lo SS, et al. Stereotactic body radiotherapy for primary prostate cancer. Technol Cancer Res Treat 2018;17:1–13. https://doi.org/10.1177/1533033818789633.
[22] Kishan AU, Dang A, Katz AJ, Mantz CA, Collins SP, Aghdam N, et al. Long-term outcomes of stereotactic body radiotherapy for low-risk and intermediate-risk prostate cancer. JAMA Netw Open 2019;2:. https://doi.org/10.1001/jamanetworkopen.2018.8006e188006.
[23] Arcangeli S, Greco C. Hypofractionated radiotherapy for organ-confined prostate cancer: is less more?. Nat Rev Urol 2016;13:400–8. https://doi.org/10.1038/nrurol.2016.106.
[24] Jiang NY, Dang AT, Yuan Y, Chu F-I, Shabsovich D, King CR, et al. Multi-institutional analysis of prostate-specific antigen kinetics after stereotactic body radiation therapy. Int J Radiat Oncol 2019;105:628–36. https://doi.org/10.1016/j.ijrobp.2019.06.2539.
[25] Lin Y, Liu T, Yang W, Yang X, Khan MK. The non-gaussian nature of prostate motion based on real-time intrafraction tracking. Int J Radiat Oncol Biol Phys 2013;87:363–9. https://doi.org/10.1016/j.ijrobp.2013.05.019.
[26] Langen KM, Willoughby TR, Meeks SL, Santhanam A, Cunningham A, Levine L, et al. Observations on real-time prostate gland motion using electromagnetic tracking. Int J Radiat Oncol Biol Phys 2008;71:1084–90. https://doi.org/10.1016/j.ijrobp.2007.11.054.
[27] Kupelian P, Willoughby T, Mahadevan A, Djemil T, Weinstein G, Jani S, et al. Multi-institutional clinical experience with the Calypso System in localization and continuous, real-time monitoring of the prostate gland during external radiotherapy. Int J Radiat Oncol Biol Phys 2007;67:1088–98. https://doi.org/10.1016/j.ijrobp.2006.10.026.
[28] Litzenberg DW, Balter JM, Hadley SW, Hamstra DA, Willoughby TR, Kupelian PA, et al. Prostate intrafraction translation margins for real-time monitoring and correction strategies. Prostate Cancer 2012;2012:1–6. https://doi.org/10.1155/2012/130579.
[29] Lovelock DM, Messineo AP, Cox BW, Kollmeier MA, Zelefsky MJ. Continuous monitoring and intrafraction target position correction during treatment improves target coverage for patients undergoing sbrt prostate therapy. Int J Radiat Oncol Biol Phys 2015;91:588–94. https://doi.org/10.1016/j.ijrobp.2014.10.049.
[30] Padhani AR, Khoo VS, Suckling J, Husband JE, Leach MO, Dearnaley DP. Evaluating the effect of rectal distension and rectal movement on prostate gland position using cine MRI. Int J Radiat Oncol Biol Phys 1999;44:525–33. https://doi.org/10.1016/S0360-3016(99)00040-1.
[31] Ghilezan MJ, Jaffray DA, Siewerdsen JH, Van Herk M, Shetty A, Sharpe MB, et al. Prostate gland motion assessed with cine-magnetic resonance imaging (cine-MRI). Int J Radiat Oncol Biol Phys 2005;62:406–17. https://doi.org/10.1016/j.ijrobp.2003.10.017.
[32] Ogino I, Kaneko T, Suzuki R, Matsui T, Tabekashi S, Inoue T, et al. Rectal content and intrafractional prostate gland motion assessed by magnetic resonance imaging. J Radiat Res 2011;52:199–207. https://doi.org/10.1269/jrr.10126.
[33] Palit S, Lunniss PJ, Scott SM. The physiology of human defecation. Dig Dis Sci 2012;57:1445–64. https://doi.org/10.1007/s10620-012-2071-1.
[34] Hobday DI, Aziz Q, Thacker N, Hollander I, Jackson A, Thompson DG. A study of the cortical processing of ano-rectal sensation using functional MRI. Brain 2001;124:361–8. https://doi.org/10.1093/brain/124.2.361.
[35] Walz J, Epstein JI, Ganzer R, Graefen M, Guazzoni G, Kaouk J, et al. A critical analysis of the current knowledge of surgical anatomy of the prostate related to optimisation of cancer control and preservation of continence and erection in candidates for radical prostatectomy: an update. Eur Urol 2016;70:301–11. https://doi.org/10.1016/j.eururo.2016.01.026.
[36] Mahieu P, Pringot J, Defecography Bodart P. I. Description of a new procedure and results in normal patients. Gastrointest Radiol 1984. https://doi.org/10.1007/BF01887845.
[37] Maccioni F. Functional disorders of the ano-rectal compartment of the pelvic floor: Clinical and diagnostic value of dynamic MRI. Abdom Imaging 2013;38:930–51. https://doi.org/10.1007/s00261-012-9955-6.
[38] Bodo S, Campagne C, Thin TH, Higginson DS, Vargas HA, Hua G, et al. Single-dose radiotherapy disables tumor cell homologous recombination via ischemia/reperfusion injury. J Clin Invest 2019;129. https://doi.org/10.1172/JCI97631.